Supporting Information

Constructing efficient and stable $CsPbBr_3$ nanocrystals via calcium and fluorine ions combined-treatment for light-emitting diodes

Mingming Liu[a], Qun Wan[b,c], Xinrong Liao[a], Wenji Zhan[a], Changwei Yuan[a], Qinggang Zhang[a], Mengda He[a], Cong Zou[a], Meitian Pan[a], Long Kong[a], Liang Li*[b,c]

[a]School of Environmental Science and Engineering, Shanghai Jiao Tong University, Shanghai 200240, China

[b]Macao Institute of Materials Science and Engineering (MIMSE), Macao University of Science and Technology, Taipa 999078 Macao, China

[c]Zhuhai MUST Science and Technology Research Institute, Zhuhai 519099, China

E-mail: lli@must.edu.mo

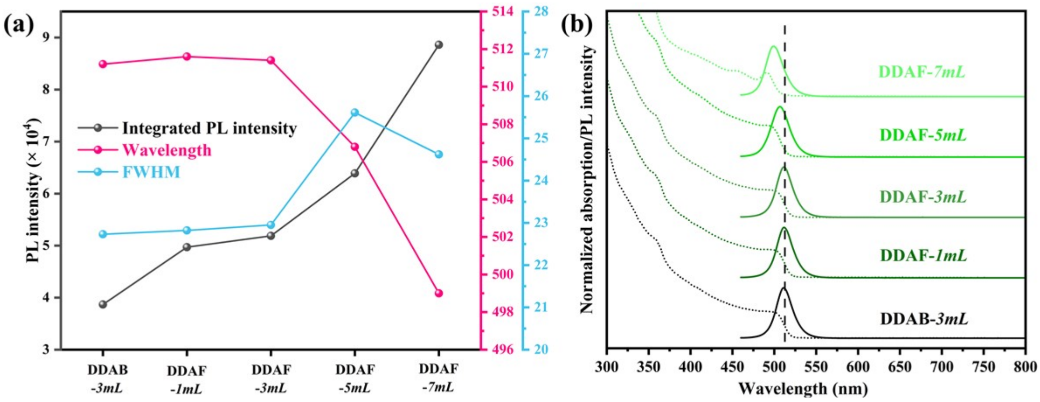

Fig. S1 (a) Optical properties of PNCs with different amount of DDAF in step one. (b) The corresponding normalized absorption and PL spectra.

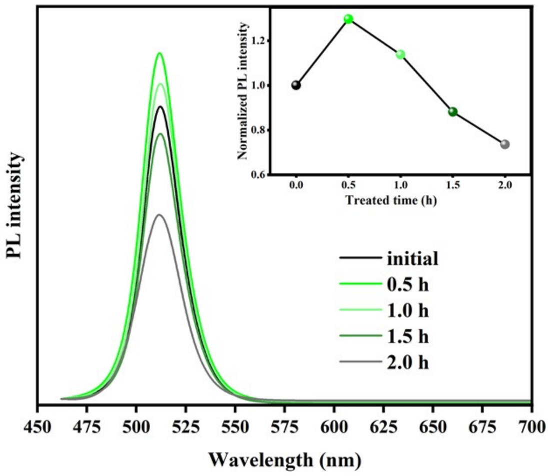

Fig. S2 The PL spectra of PNCs with different treated time in step two. (The inset represents the corresponding PL intensity changes.)

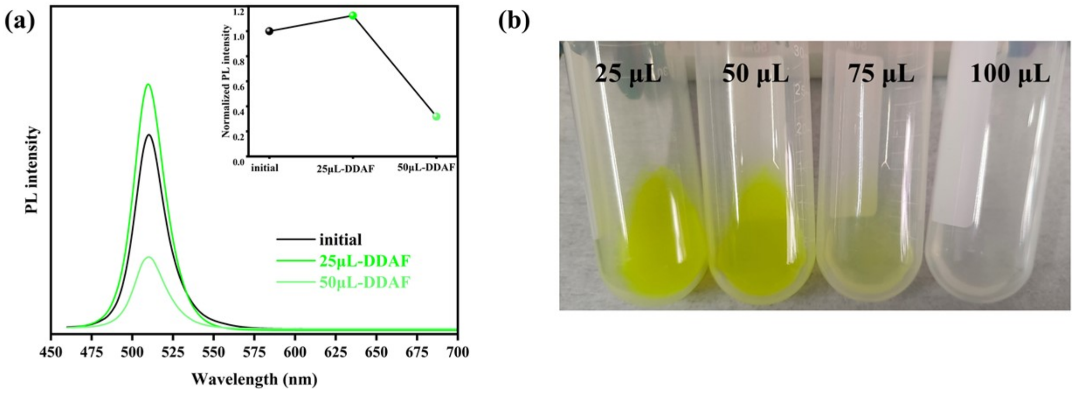

Fig. S3 (a) The PL spectra of PNCs treated with different amount of DDAF in step three. (The inset represents the corresponding PL intensity changes.) (b) The ambient light images of different DDAF treated PNCs with adding anti-solvent in step three.

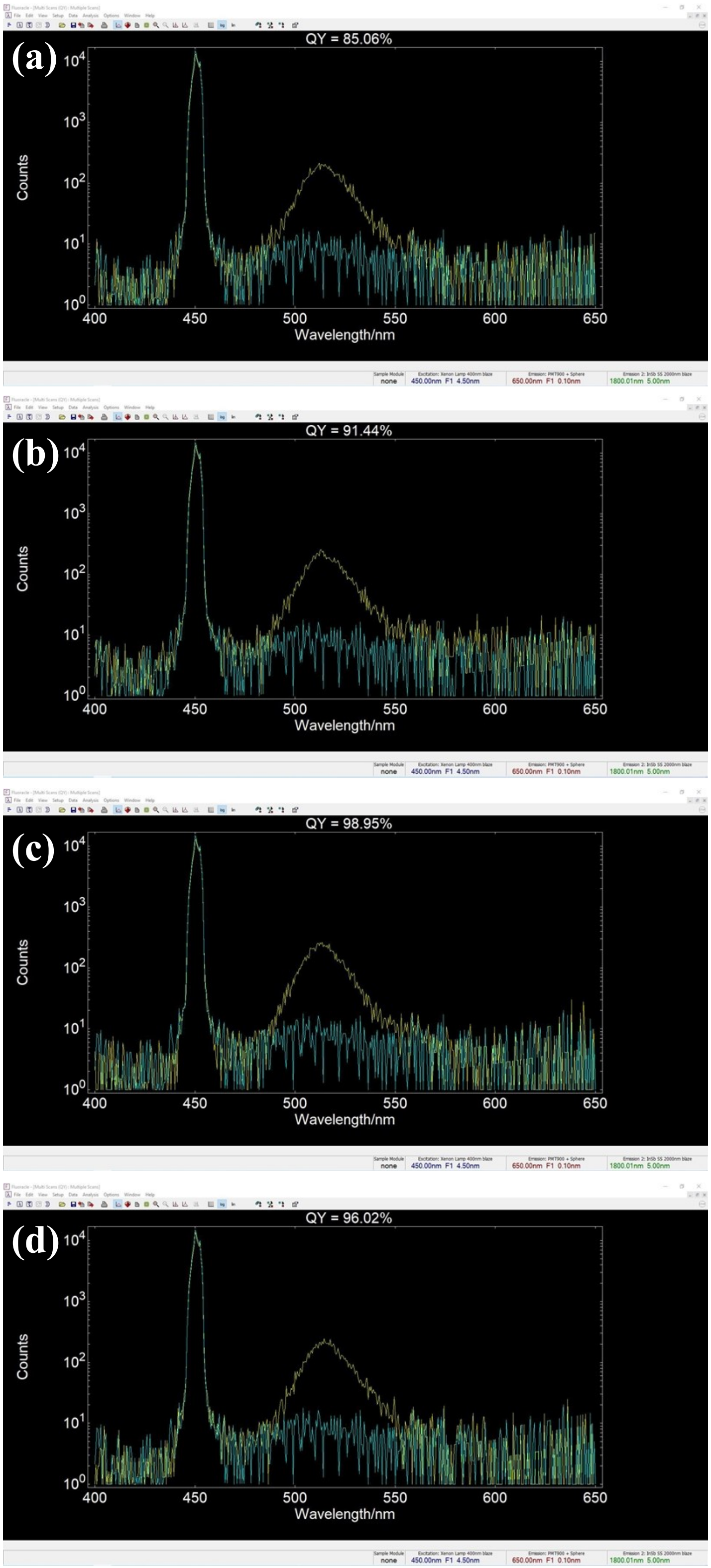

Fig. S4 Photographs of photoluminescence efficiency of (a) $CsPbBr_3$, (b) $CsPbBr_3$@F, (c) $CsPbBr_3$@F·Ca and (d) $CsPbBr_3$@F·CaF PNCs.

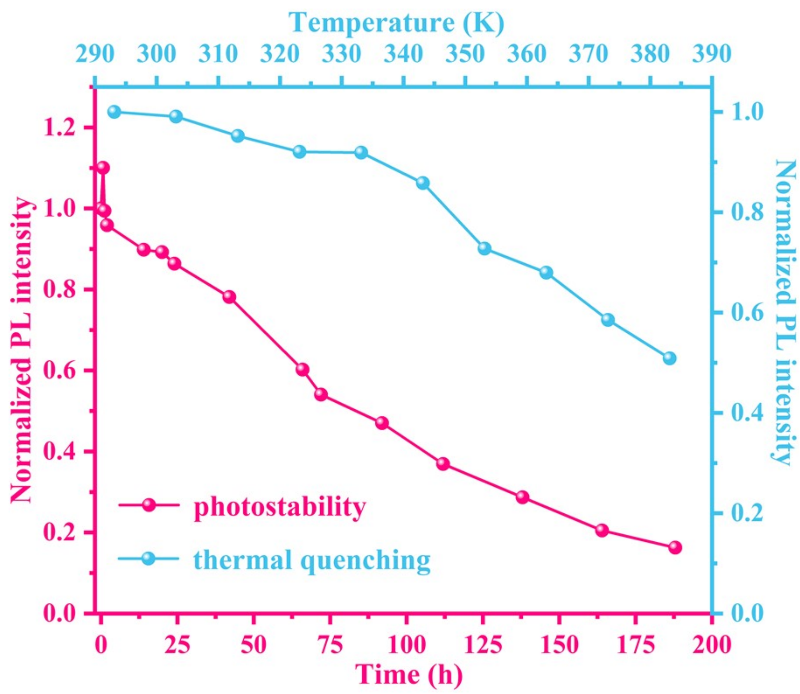

Fig. S5 The photostability and thermal quenching curves of $CsPbBr_3$ PNCs

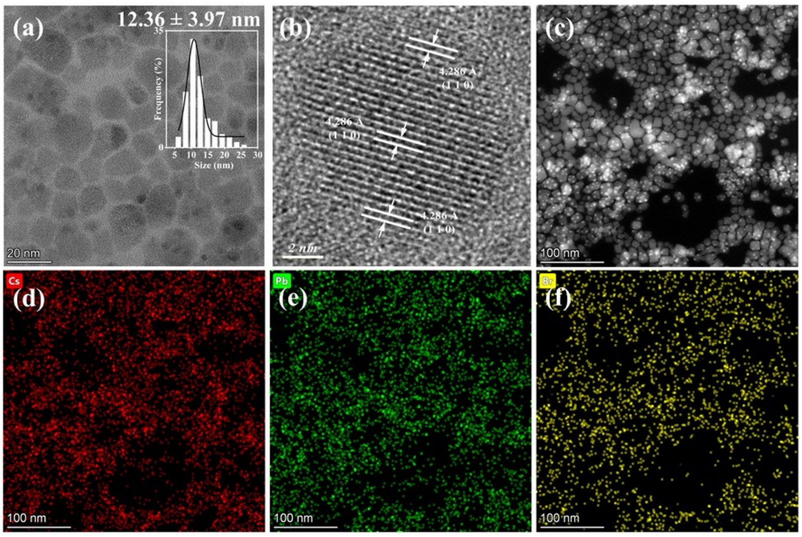

Fig. S6 (a) TEM (inset was the corresponding size distribution), (b) HRTEM, (c) HAADF-STEM and the corresponding elemental mapping of (d) Cs, (e) Pb and (f) Br of $CsPbBr_3$ PNCs.

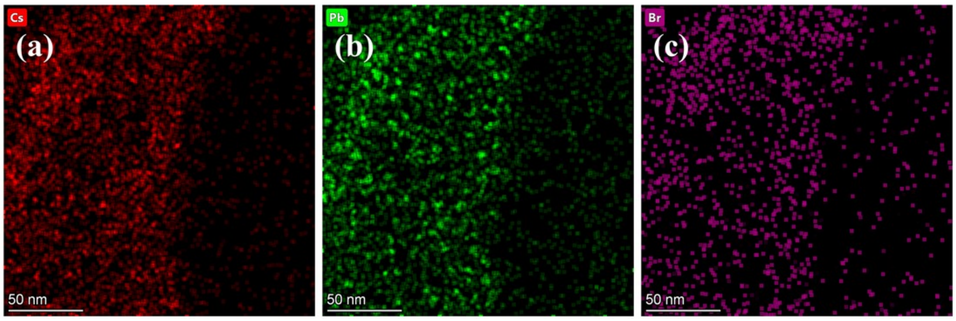

Fig. S7 The elemental mapping of Cs, Pb and Br in a $CsPbBr_3$@F·CaF PNC sample.

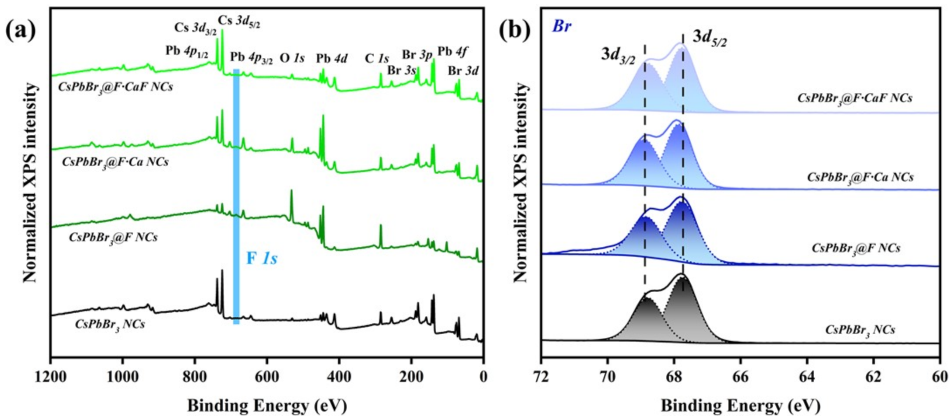

Fig. S8 (a) XPS survey spectra and (b) high-resolution XPS spectra of Br 3*d* of $CsPbBr_3$, $CsPbBr_3$@F, $CsPbBr_3$@F·Ca and $CsPbBr_3$@F·CaF PNCs.

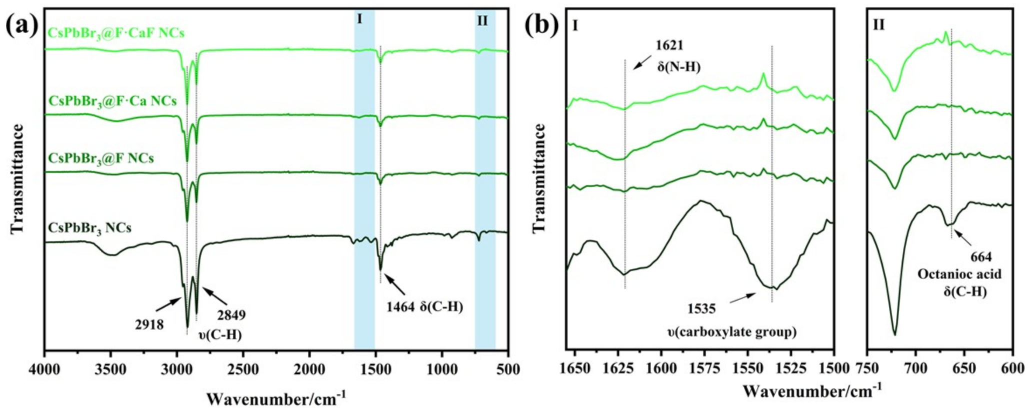

Fig. S9 (a) FTIR of $CsPbBr_3$, $CsPbBr_3$@F, $CsPbBr_3$@F·Ca, $CsPbBr_3$@F·CaF nanocrystals. (b) The enlarged images of area I and II of picture (a).

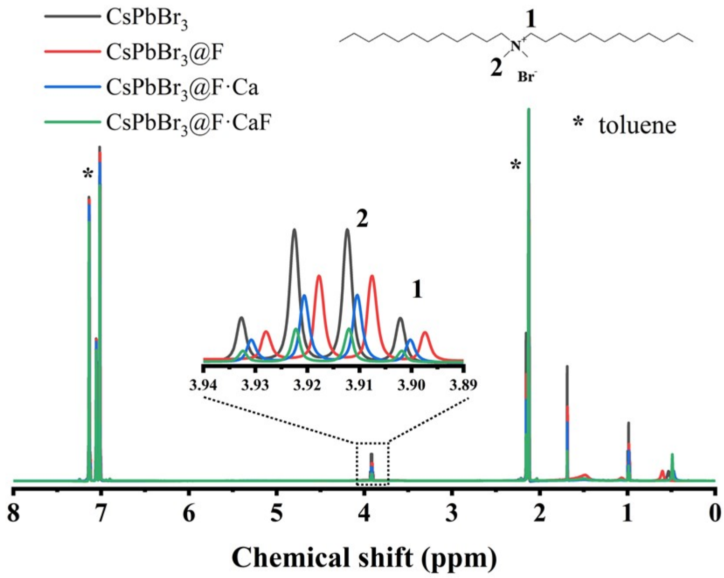

Fig. S10 [1]H NMR of $CsPbBr_3$, $CsPbBr_3$@F, $CsPbBr_3$@F·Ca, $CsPbBr_3$@F·CaF PNCs.

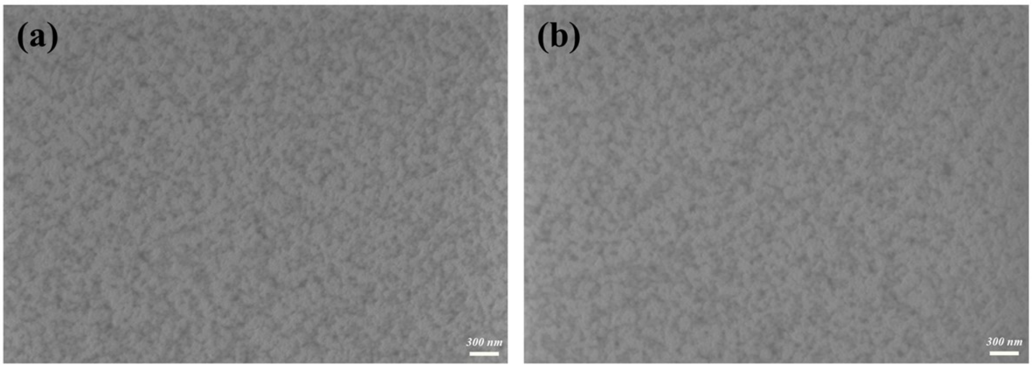

Fig. S11 SEM images of (a) $CsPbBr_3$@F and (b) $CsPbBr_3$@F·CaF films.

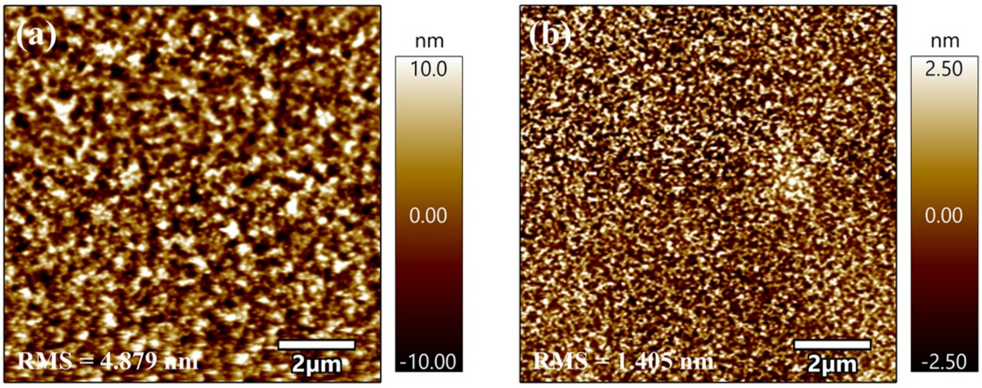

Fig. S12 AFM images of (a) $CsPbBr_3$@F and (b) $CsPbBr_3$@F·CaF films.

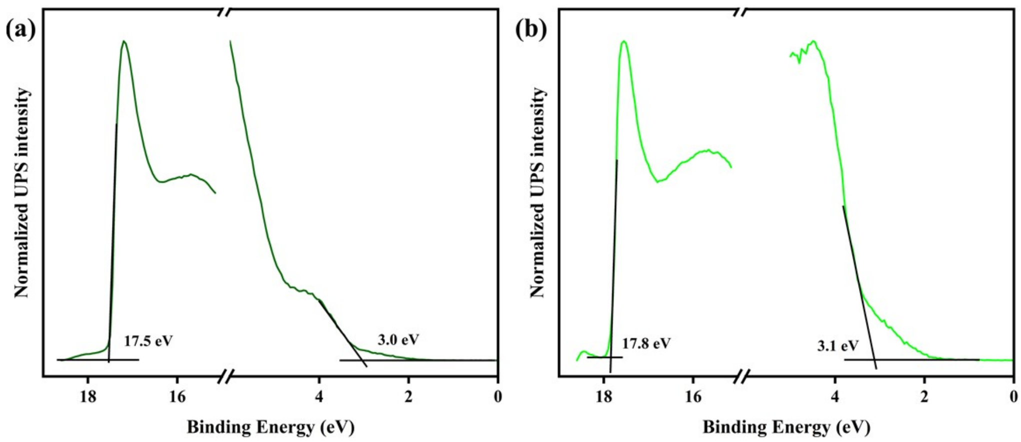

Fig. S13 UPS spectra of (a) $CsPbBr_3$@F and (b) $CsPbBr_3$@F·CaF PNCs samples.

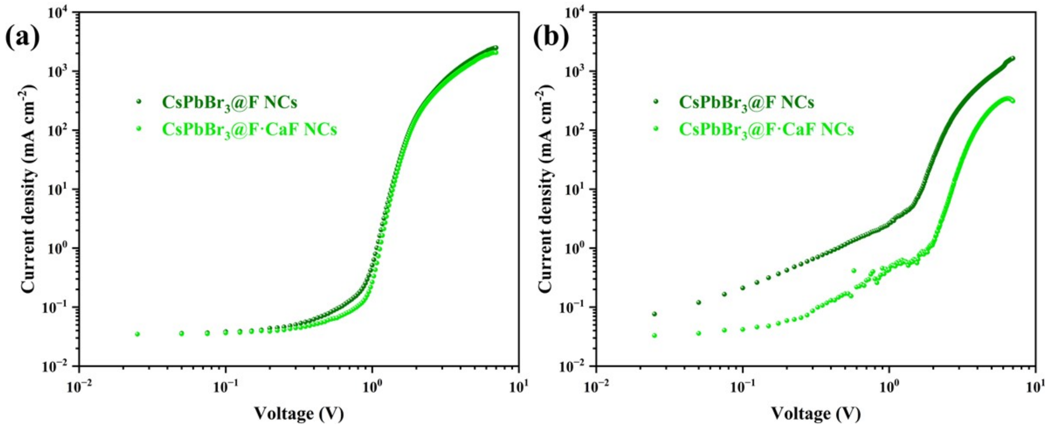

Fig. S14 Current density as a function of voltage in (a) hole-only and (b) electron-only devices.

Table S1 Summary of time-resolved PL bi-exponential fitting parameters for solutions of the PNCs.

Samples	A_1 (%)	τ_1 (ns)	A_2 (%)	τ_2 (ns)	$\tau_{avg.}$ (ns)	A_1' (%)	A_2' (%)	Φ (%)	K_r (μs^{-1})	K_{nr} (μs^{-1})
$CsPbBr_3$	76.86	7.80	21.50	25.88	16.50	51.86	48.14	85.06	51.54	9.05
$CsPbBr_3$@F	85.55	6.96	16.22	24.54	14.00	59.95	40.05	91.44	65.29	6.11
$CsPbBr_3$@F·Ca	87.51	6.52	14.66	17.36	9.86	69.15	30.85	96.02	97.36	4.04
$CsPbBr_3$@F·CaF	96.81	6.61	6.91	19.50	8.85	82.60	17.40	98.95	111.77	1.19

Note:

(1) A and τ are the amplitude and decay time constant respectively. τ_{avg} is calculated as

$$\tau_{avg} = \frac{A_1\tau_1^2 + A_2\tau_2^2}{A_1\tau_1 + A_2\tau_2}$$

(2) A_x' represented the proportion of τ_x, recalculated as

$$A_x^{'} = \frac{A_x\tau_x}{A_1\tau_1 + A_2\tau_2} \quad \mathbf{x = 1\ or\ 2}$$

(3)

$$\Phi = \frac{k_r}{k_r + k_{nr}} \quad \tau_{avg.} = \frac{1}{k_r + k_{nr}}$$

k_r represents radiative combination rate

k_{nr} represents nonradiative combination rate